River Flow 2010 - Dittrich, Koll, Aberle & Geisenhainer (eds) - © 2010 Bundesanstalt für Wasserbau ISBN 978-3-939230-00-7

Shallow-water model with porosity: sensitivity analysis to head losses and porosity distribution

M. Velickovic
Fonds pour la formation à la Recherche dans l'Industrie et dans l'Agriculture – FRIA, Dept. Of Civil and Environmental Engineering, Université catholique de Louvain, B-1348 Louvain-la-Neuve, Belgium

S. Van Emelen & Y. Zech
Dept. Of Civil and Environmental Engineering, Université catholique de Louvain, B-1348 Louvain-la-Neuve, Belgium

S. Soares-Frazão
Fonds de la Recherche Scientifique – FNRS, Dept. Of Civil and Environmental Engineering, Université catholique de Louvain, Louvain-la-Neuve, Belgium

ABSTRACT: The shallow-water model with porosity is an attractive and efficient way to simulate inundations in valleys with urbanised areas. Indeed, at a very large scale, an urbanised area can be compared to a porous media, for which the porosity parameter is the ratio between the space available for the flow (i.e. the streets) and the total area. The urban fabric is also characterised by eddy head losses. The first part of this paper is devoted to the sensitivity analysis of the model to these head losses by comparing numerical results with experimental data, in steady and transient flow. It is shown that this coefficient is necessary to represent accurately the flow through the urbanized zone, although beyond a certain threshold, it has no more influence on the results. Then, the distribution of the porosity parameter is investigated. Indeed, in former works it was always considered that this parameter was homogenous inside the urbanized area, and that its value varied discontinuously at its boundaries. In the present study, a linearly-varied distribution is tested. It is shown that in certain cases, smoothing the distribution of the porosity can improve the results.

Keywords: Flood modelling, Urban flooding, Porosity, Head losses, Porosity distribution

1 INTRODUCTION

The simulation of floods in urban areas is important to assess the risks or to draw emergency plans. However, it is a difficult task because of the complexity of the flow through such a media, and because of the scale of the problem. Indeed, simulating the flow in details in each street would be tedious or even impossible due to lack of data. That is why in the last decade, 2D simplified models were developed to overcome this difficulty (McMillan 2007). Among them, a promising approach is to represent the urban fabric as a porous medium (Lhomme 2006, Guinot and Soares-Frazão 2006, Soares-Frazão et al. 2008, Sanders et al. 2008).

Indeed, at a large scale (Figure 1), the urban fabric can be assimilated to a 2D porous medium, in which the streets are the pores, and the buildings are the obstacles. As illustrated in Figure 1, this medium is often not homogeneous and presents anisotropy, due to the presence of wide and long avenues that form preferential paths for the flow.

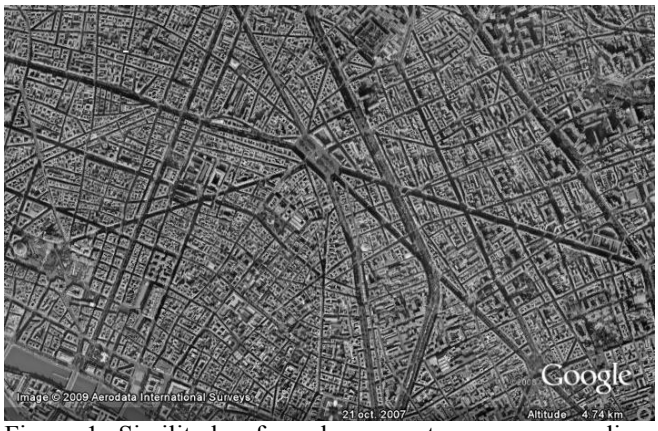

Figure 1: Similitude of a urban area to a porous medium (Paris, France Google Earth)

The porosity approach leads to modified shallow-water equations including a porosity parameter to account for the area available to the flow in a given control volume. Specific eddy losses terms are then added to account for the important flow fluctuations induced by the successive widenings and constrictions of the flow through the urban area. Soares-Frazão et al. (2008) propose a Borda-type formulation, while Sanders et al. (2008) propose to quantify the eddy losses by means of a drag coefficient.

To solve the porosity equations, Guinot and Soares-Frazão (2006) proposed a finite-volume scheme with LHLL-type fluxes. This scheme was successfully tested in several unsteady or dam-break flow situations but no steady-flow validations are yet reported. Among the dam-break flow tests, experiments in an idealised urban district (Soares-Frazão and Zech 2008) were used.

In this paper, we present new steady-flow experiments performed in the idealised urban district configuration used by Soares-Frazão and Zech (2008). The porosity model by Guinot and Soares-Frazão (2006) will be tested against these new data. A sensitivity analysis to the head-loss coefficient is performed on both dam-break and steady-flow cases. Then, the influence of the porosity distribution is analysed.

2 EXPERIMENTS

2.1 *Experimental set-up*

Two types of experiments are described in this paper. The first ones are transient flow experiments, and were conducted by Soares-Frazão and Zech (2008). The second ones were carried out in the same set-up but in steady-flow conditions (Van Emelen 2009).

The experiments were conducted at the Hydraulics Laboratory of the Civil and Environmental Engineering Department of the Université catholique de Louvain, Belgium. The channel is 36 m long and 3.6 m wide, with a partly trapezoidal cross section as indicated in Figure 2. From former measurements, the channel Manning roughness coefficient was estimated at 0.01 $sm^{-1/3}$.

A gate separates an upstream reservoir from the downstream channel. The gate is located between two impervious blocks in order to simulate transient flows through a rectangular breach. This dam-break flow is generated with an initial water level in the reservoir of 0.40 m and a thin layer of 0.011 m water in the downstream reach. On the other hand, steady flows are generated by pumping downstream water and re-circulating it upstream, the gate being left open. In the present experiments, the discharge is 100 l/s, and a weir is placed at the downstream end of the channel to force a subcritical flow with a depth of about 0.20 m.

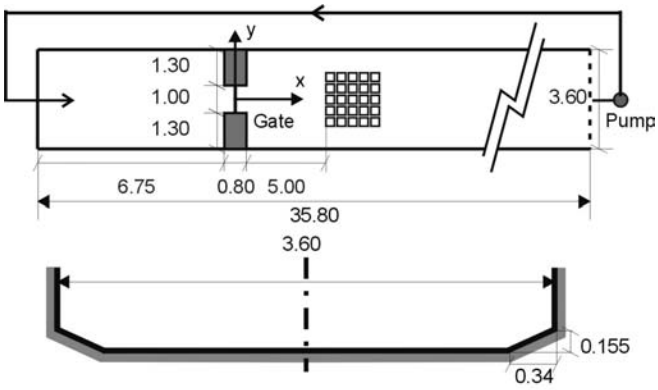

Figure 2: Experimental set-up: channel dimensions (m)

The simplified urban district in the experiments is composed of 5×5 wooden blocks aligned with the flow direction (Figure 2). The "city" is placed at the centre of the channel section, 5 m downstream of the gate. The "buildings" dimensions are 0.3 m × 0.3 m, while the "streets" are 0.1 m wide. The buildings are fixed on the channel bed using a no-slip material at the bottom and heavy weights inside the blocks.

2.2 *Measurement devices*

Several measurement devices were used to characterise the flow. These devices differ in the dam-break flow and in the steady flow experiments.

The water level evolution in dam-break flows was measured by means of several resistive gauges. Figure 3a shows the locations of the gauging points (about 40 gauge locations over the channel). Thanks to the repeatability of the experiment (Soares-Frazão and Zech 2008), those water level measurements can be combined to form water profiles in the streets. In the steady-flow case, the water level (which is constant in time) is measured with ultrasonic gauges fixed on a moving device to measure continuous water profiles along the "streets" (Figure 3b).

For both flow cases, the surface velocity field was obtained using digital imaging techniques (Capart et al. 2002, Spinewine et al. 2003) by tracking the movement of tracer particles on the free surface. Again, thanks to the repeatability of the experiment, several locations could be imaged and combined, which allows to identify particular features of the flow such as re-circulation for example. The study areas for the velocity field in the transient and steady flow cases are indicated in Figure 4.

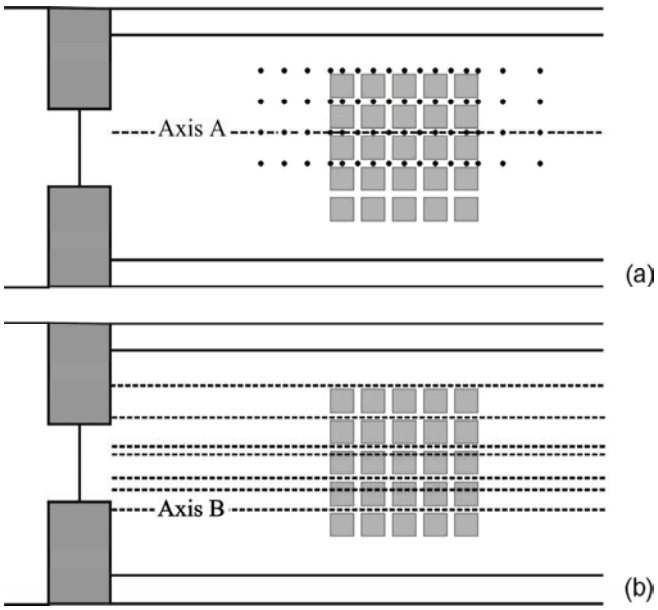

Figure 3: (a) Positions of the gauging points for transient flow; (b) location of water profiles for steady flow (not at scale)

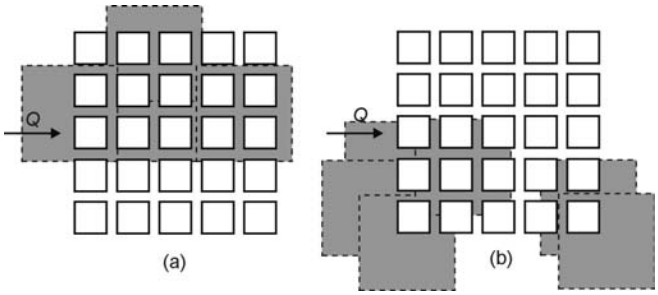

Figure 4: Areas filmed in experiments: (a) transient flow and (b) steady flow

2.3 *Transient flow description*

In the dam-break case, two main phenomena can be observed. After the strong impact of the wave against the buildings, the flow slows down before entering the streets. A hydraulic jump forms upstream of the city entrance (Figure 5), with the consequence that the water level is locally higher than without buildings. Immediately downstream of the city, a wake zone is observed. Then, further downstream, the flow slowly recovers the structure it would have had without the presence of the city (Soares-Frazão et al. 2008).

2.4 *Steady flow description*

The steady flow experiment is less spectacular than the dam-break flow. Indeed, the consequences of the presence of the city are less immediately visible. However, a small increase of the water level can be observed just upstream of the city (Figure 6), which is immediately followed by a small decrease just after the entrance into the city. In the same way, flow observations show a little decrease of the water level at the exit of the city.

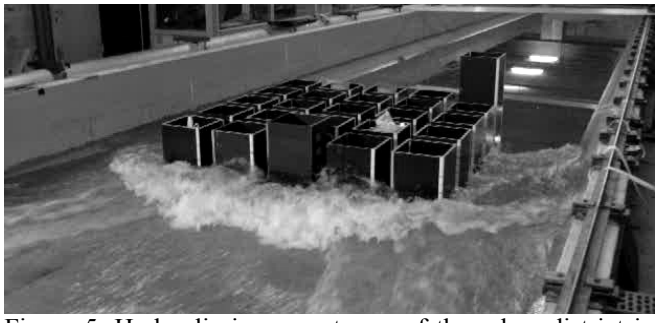
Figure 5. Hydraulic jump upstream of the urban district in transient case


Figure 6. Small variation of the water level at the city entrance

3 GOVERNING EQUATIONS AND NUMERICAL SCHEME

3.1 *The porosity model*

Defining the porosity ϕ as the ratio between the plan-view area available to the flow to the whole urban district area, the 2D shallow water equations with porosity can be written in conservation form as (Soares-Frazão et al. 2008)

$$\frac{\partial \mathbf{U}}{\partial t}+\frac{\partial \mathbf{F}}{\partial x}+\frac{\partial \mathbf{G}}{\partial y}=\mathbf{S} \qquad (1)$$

where

$$\mathbf{U}=\begin{pmatrix}\phi h\\ \phi uh\\ \phi vh\end{pmatrix},\ \mathbf{F}=\begin{pmatrix}\phi uh\\ \phi u^2h+\phi\dfrac{gh^2}{2}\\ \phi uvh\end{pmatrix},$$

$$\mathbf{G}=\begin{pmatrix}\phi vh\\ \phi uvh\\ \phi v^2h+\phi\dfrac{gh^2}{2}\end{pmatrix}$$

$$\text{and } \mathbf{S} = \begin{pmatrix} 0 \\ \phi\, gh\left(S_{0x} - S_{lx}\right) + \dfrac{gh^2}{2}\dfrac{\partial \phi}{\partial x} \\ \phi\, gh\left(S_{0y} - S_{ly}\right) + \dfrac{gh^2}{2}\dfrac{\partial \phi}{\partial y} \end{pmatrix} \quad (2)$$

where ϕ is the porosity, h the water depth, u and v the depth-averaged velocities in x- and y- directions, S_{0x} and S_{0y} the bed slopes and $S_{l,x}$ and $S_{l,y}$ the head loss slopes in each direction. These last terms include friction and eddy losses:

$$S_{l,x} = \left[S_{f,x} + \frac{1}{L}\zeta \frac{(u^2+v^2)^{1/2}\, u}{2g} \right] \phi\, gh$$
$$S_{l,y} = \left[S_{f,y} + \frac{1}{L}\zeta \frac{(u^2+v^2)^{1/2}\, v}{2g} \right] \phi\, gh \quad (3)$$

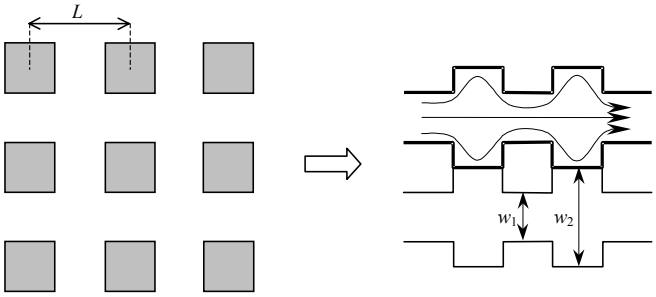

Figure 7 . Definition of distributed Borda-type head losses

In (3), $S_{f,x}$ and $S_{f,y}$ are calculated by means of the Manning formula while ζ is the Borda-type head-loss coefficient and L is the spatial period of the widening and narrowing (Figure 7).

To summarise, two terms in the governing equations account for the restriction in area available to the flow: (1) the porosity ϕ and the related porosity variation $\partial\phi/\partial x$ and $\partial\phi/\partial y$, in the source terms, and (2) the Borda-type head-loss term. In the applications, the influence of each of these terms will be investigated.

3.2 *Numerical scheme*

A finite-volume discretisation is used to solve the governing equations

$$\mathbf{U}_i^{n+1} = \mathbf{U}_i^n - \frac{\Delta t}{A_i} \sum_{j \in N(i)} \left(\mathbf{T}_{i,j}\, \mathbf{F}_{i,j}^{n+1/2}\, w_{i,j} \right) + \mathbf{S}_i^n \Delta t \quad (4)$$

where $\mathbf{U}_i^n$ is the average value of $\mathbf{U}$ over the cell i at the time level n, A_i is the area of the cell i, $\mathbf{F}_{i,j}^{n+1/2}$ is the average value of the flux vector along the normal to the interface (i,j) between the time levels n and $n+1$, $N(i)$ is the set of neighbour cells of the cell i, $\mathbf{T}_{i,j}$ is the matrix that accounts for the co-ordinate rotation from the global (x, y) coordinate system to the local system attached to the interface, $\mathbf{S}_i^n$ is the average value over the cell i between the time levels n and $n+1$ of the source term, $w_{i,j}$ is the length of the interface (i,j) and Δt is the computational time step.

The fluxes are calculated by a HLL-type solver (Guinot and Soares-Frazão 2006) with a lateralised discretisation for the pressure source term in the momentum equations (Fraccarollo et al. 2003). This consists in a kind of upwinding as presented by Bermudez and Vasquez (1994).

4 SENSITIVITY ANALYSIS

4.1 *Head-loss coefficient*

In the original work by Lhomme (2006), the Borda-type head loss coefficient ζ for the idealised urban district case was calibrated manually to the value of 24, with $L = 0.4$ m. This calibration was done for a dam-break flow situation.

Here, the adequacy of this calibrated value is checked in the steady-flow situation, and the sensitivity to this coefficient is investigated. According to the urban district layout, the corresponding porosity coefficient is $\phi = 0.38$. In the numerical simulation, this value is prescribed to the computational cells located in the urban area, as illustrated in Figure 8. Outside the urban district, the whole room is available to the flow, so the porosity may be defined as $\phi = 1$.

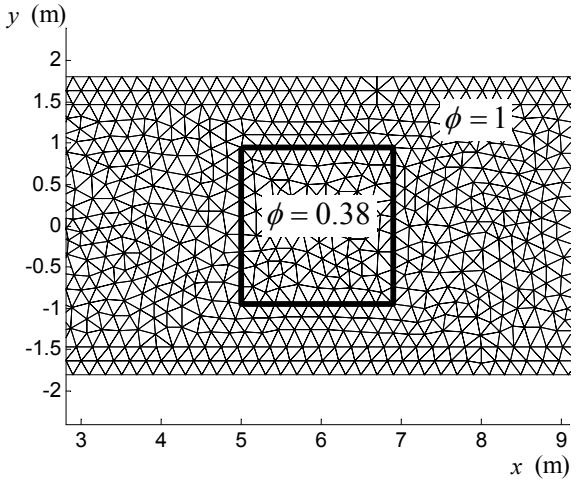

Figure 8. Computational mesh around the urban district

The tested values for the ζ head-loss coefficients are: 0, 0.784, 24 and 784, respectively. The 0 value is used to assess the influence of the porosity-related terms only, while higher value of ζ account for the additional head losses in the urban district arising from the succession of narrowing and widening in the urban district as illustrated in Figure 7. The value of 24 is the value that was calibrated by Lhomme (2006) for the dam-break flow case.

Figures 9a and b present the results for the steady-flow along the axis B (Figure 3b). Experimental results are presented as a continuous line because a continuous profile was acquired by moving the sensor over the whole channel length (Figure 3b). Figures 9c and d present the results for the dam-break flow case at $t = 10$ s along the axis A (Figure 3a). Here, experimental results recorded during the whole duration of the dam-break flow were obtained at 15 locations along axis A, yielding 15 measurement points in the profile (Figure 3a), represented by dots.

It can be observed that with $\zeta = 0$ (Figures 9a and 9c), sharp discontinuities appear at the entrance and at the exit of the urban district, this trend being more significant in the steady-flow case, even leading to unrealistic results. It can also be observed in the steady-flow case (Figure 9a) that the total head loss induced by the urban district is underestimated as the water level upstream from the urban district is much lower than the actual one.

For increasing ζ values, it can be observed that almost no more changes occur from the value $\zeta = 24$ (Figures 9b and 9d). This latter value appears to be the best suited value for both cases.

The computed and measured velocity fields around the urban district are illustrated in Figures 10 and 11. These provide interesting information on the influence of the ζ coefficient. For $\zeta = 0$, it appears that the flow is accelerated through the urban district, which is the contrary of the expected behaviour. This abrupt acceleration is induced by the $\partial\phi/\partial x$ and $\partial\phi/\partial y$ source terms, for which the effect is concentrated on the computational cells located on both sides of the urban district perimeter, where the porosity jumps from 1 to 0.38. The abrupt flow acceleration is stronger in the steady-flow case. In the dam-break flow case, the dynamic effect of the flow impact against the virtual wall induced by the porosity discontinuity smoothens out the velocity variation.

In both the steady and dam-break flow cases, it can be observed that an increasing ζ value has the positive effect of slowing down the flow through the urban district. This is coherent with the experimental observation (Figure 10e for the steady-flow case) where the velocity vectors direction indicates that the major part of the flow passes outside the urban district.

From the velocity vectors in Figure 10c and 10d, we can conclude that flow velocity reduction through the city is such that even a very high ζ value will not significantly affect the amplitude of the corresponding source term in expression (3).

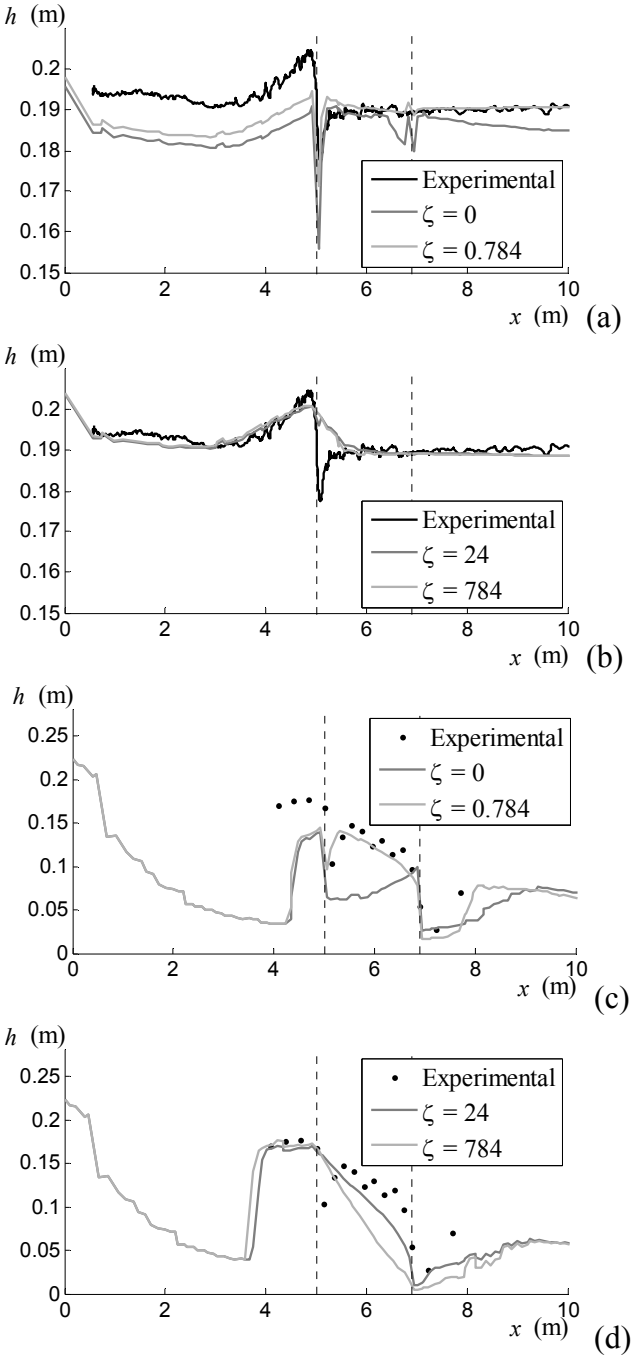

Figure 9: Comparison between experimental and numerical water levels, (a and b) in steady flow along the axis B defined in Figure 3b (y = -0.6 m), and (c and d) in dam break flow along the axis A as defined in Figure 3a (y = 0.2 m).

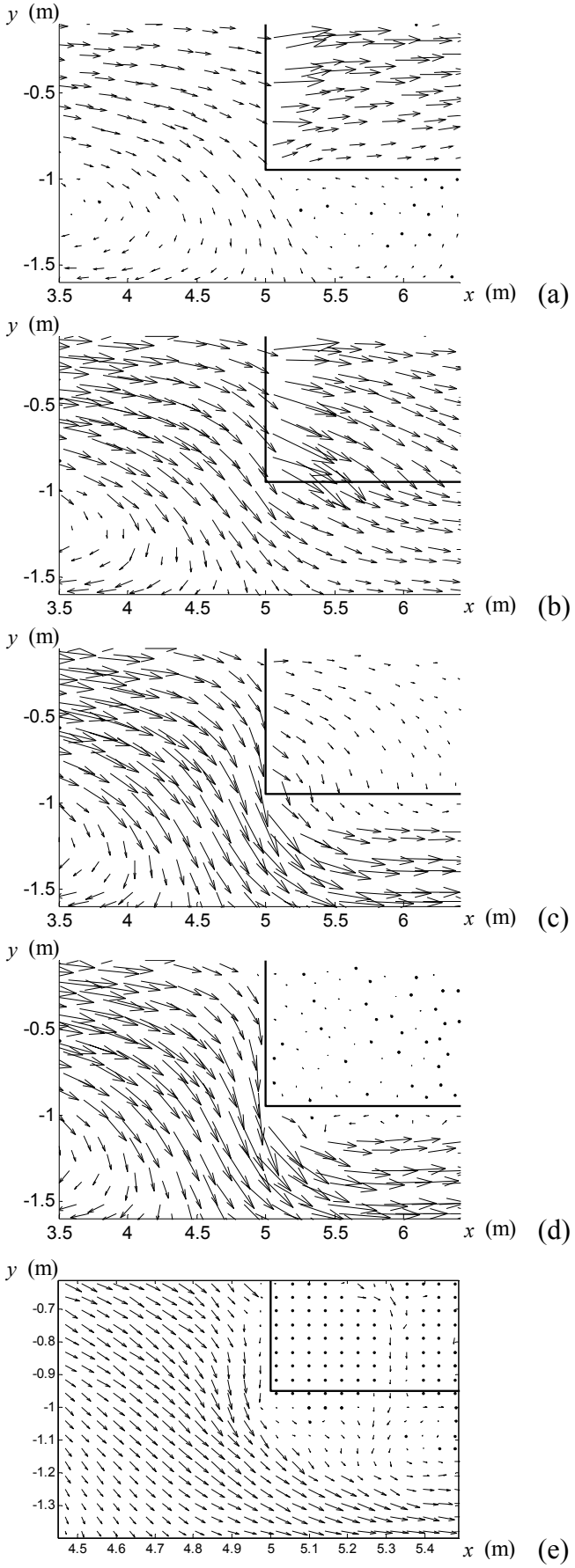

Figures 10: Computed velocity fields around the urban district in steady flow, with (a) ζ=0, (b) ζ=0.784, (c) ζ=24, (d) ζ=784, and (e) measured water velocity, around the south-west corner of the urban area.

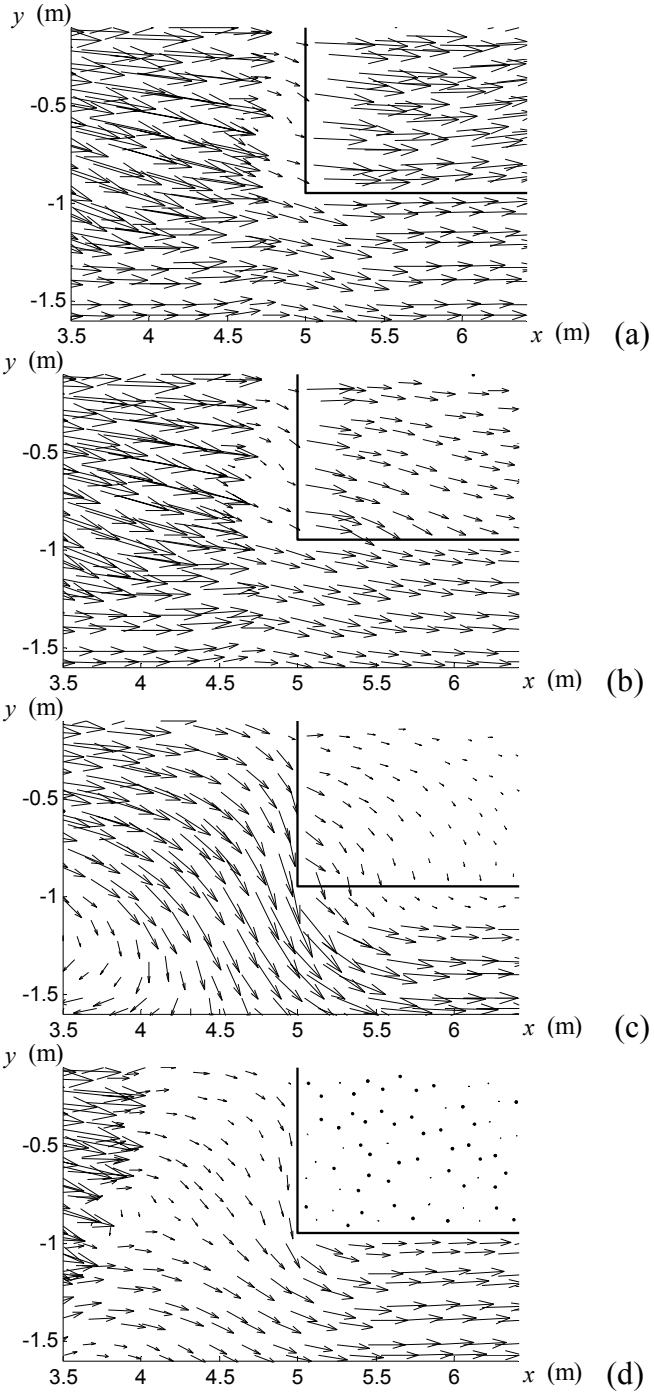

Figures 11: Computed velocity fields around the urban district in dam-break flow, with (a) ζ=0, (b) ζ=0.784, (c) ζ=24, (d) ζ=784, around the south-west corner of the urban area.

4.2 *Porosity distribution*

It can be observed in Figure 9a that a sharp porosity discontinuity induces sharp and unrealistic water-level discontinuities, especially in the steady-flow case. If we consider that one of the effects of the presence of the urban district is to reduce the area available to the flow, we can to a certain extent make an analogy with a sudden flow constriction. In such a case, for which the classical Borda head losses apply, the flow adapts itself to smoothen the abrupt channel narrowing, leading to the well known *vena contracta*. This means that

the abrupt channel narrowing is replaced by a progressive narrowing.

Applying a similar reasoning to the idealized urban district, we could consider that the change in porosity is distributed in a progressive way. In a first trial, a linear distribution is adopted as illustrated in Figure 12.

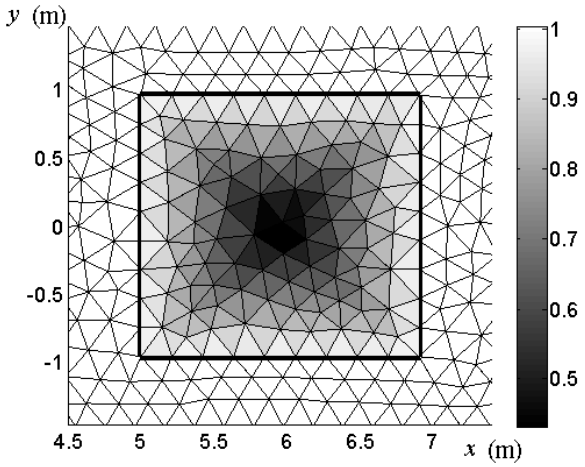

Figure 12. Linear distribution of the porosity in the urban district.

The computed results are shown in Figures 13 to 16, with $\zeta = 0$ (Figures 13 and 14) and $\zeta = 24$ (Figures 15 and 16), in steady and dam-break flow. In the figures showing water levels, the results computed with the uniform porosity distribution are also represented.

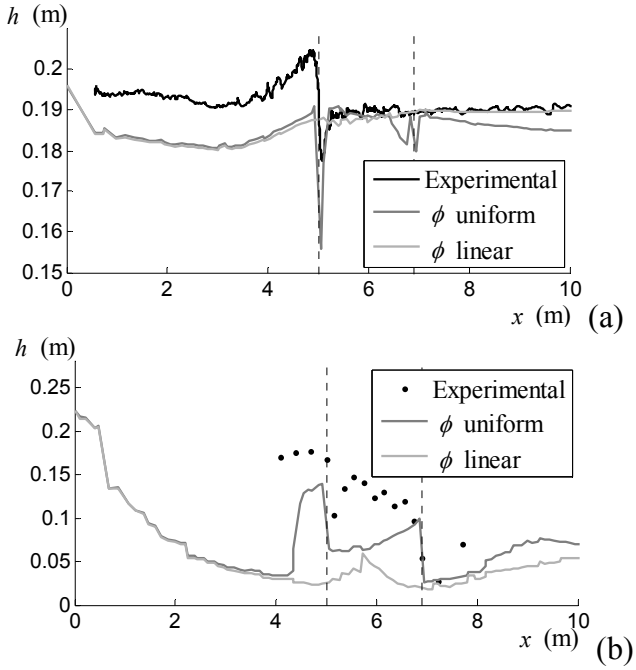

Figure 13: Water levels for uniform and linear distribution of ϕ, $\zeta = 0$, (a) in steady flow along the axis B and (b) dam-break flow along the axis A

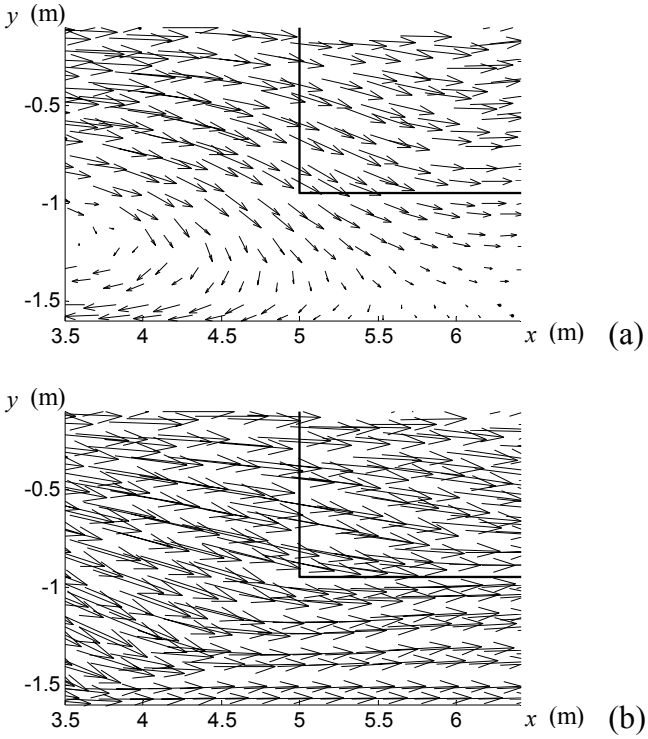

Figure 14: Velocity fields for uniform and linear distribution of ϕ, $\zeta = 0$, (a) in steady and (b) in transient flow.

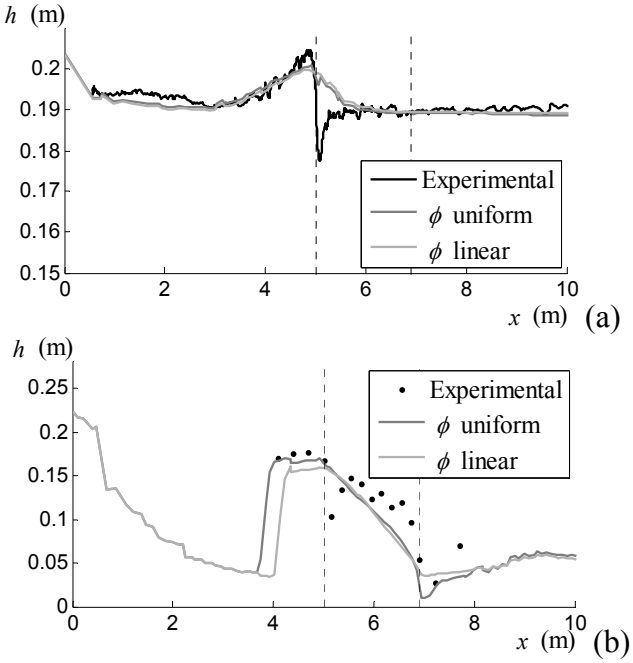

Figure 15: Water levels for uniform and linear distribution of ϕ, $\zeta = 24$, (a) in steady flow along the axis B and (b) dam-break flow along the axis A

For the case with $\zeta = 0$, a significant improvement of the quality of the results is observed in the steady-flow case (Figure 13a): the sharp water-level discontinuities disappear. However, the total head loss induced by the urban district is underestimated. In the dam-break flow case (Figure 13b), the results with the distributed porosity are worst than with the uniform porosity. This is confirmed by the velocity vectors: only a very weak flow deviation is induced by the urban district (Figure 14b).

If we consider the combination of the Borda-type head losses with $\zeta = 24$, the results illustrated in Figures 15 and 16 are obtained. In steady-flow, almost no difference between the results can be observed, while in dam-break flow, the hydraulic jump upstream of the urban district is delayed.

Looking at the velocity vectors (Figure 16) confirms that the velocity reduction in the urban district induced by the head-loss coefficient significantly changes the whole velocity distribution. The major part of the flow now passes around the urban district.

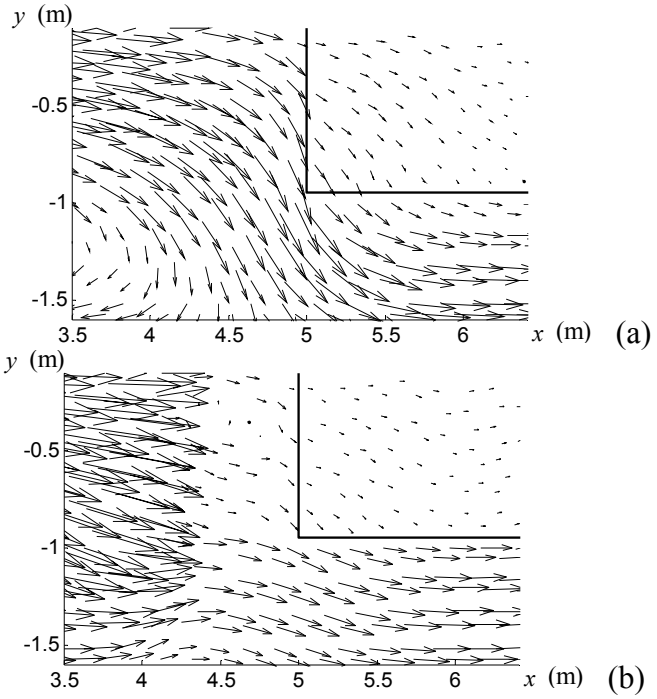

Figure 16: Velocity fields for uniform and linear distribution of ϕ, $\zeta = 24$, (a) in steady and (b) in transient flow.

5 CONCLUSION

This paper focuses on flood flow through urbanized areas. Two experiments in an idealised city are considered, one in steady-flow conditions, the other one featuring a dam-break wave. The water depth and the velocity field at defined points were measured. These experimental measurements were compared to the numerical results of a porosity model, solved by the finite-volume method. It was shown that as far as an eddy head-loss is added to the model, this latter was able to represent accurately the flow.

A sensitivity analysis to the coefficient used for expressing this head-loss showed that over a certain value, its effect on the flow did not change anymore. Then, a study of the distribution of the porosity was proposed. Two configurations of the porosity were considered: a discontinuous one where the porosity abruptly varies at the boundaries of the urban fabric, and a linear distribution in form of a pyramid with a minimum value at the city centre. It was shown that when no eddy head-loss coefficient was used, the pyramidal distribution gave more realistic results in steady flow case, while in transient state, the results may become worse. In this transient case, more sophisticated porosity distributions should improve the results. When the calibrated head-loss coefficient was applied, both configurations gave similar results, close to the experimental results. But with this calibrated head-loss coefficient, the computed velocity fields showed that the flow was rejected outside the urban area, to an exaggerated extent.

REFERENCES

Bermùdez, A., Vázquez, M.E. 1994. Upwind methods for hyperbolic conservation laws with source terms. Computers and Fluids, 23(8), 1049-1071.

Braschi, G., Gallati, M. 1992. A conservative flux prediction algorithm for the explicit computation of transcritical flow in natural streams. Hydraulic Engineering Software IV : Fluid flow modelling, Computational Mechanics Publications, Southampton, 381-394.

Fraccarollo, L., Capart, H., Zech, Y. 2003. A Godunov method for the computation of erosional shallow water transients. Internat. J. Numer. Method. Fluid. 41, 951-976.

Capart, H., Young, D.L., Zech, Y. 2002. Voronoï imaging methods for the measurements of granular flows. Experiments in Fluids, 32(1), 121-135.

Guinot, V., Soares-Frazão, S. 2006. Flux and source term discretization in two-dimensional shallow water models with porosity on unstructured grids. Int J. Numer. Meth. Fluids 2006, 50, 309-345; DOI: 10.1002/fld.1059.

Lhomme J. 2006. Modélisation des inondations en milieu urbain: approches unidimentionnelle, bidimentionelle et macroscipoque. PhD thesis, Université Montpellier II.

McMillan, H.K., Brasington, J. 2007. Reduced complexity strategies for modeling urban floodplain inundation. Geomorphology, 90, 226-243;

Sanders, B.F., Schubert, J.E., Gallegos, H.A. 2008. Integral formulation of shallow-water equations with anisotropic porosity for urban flood modeling. Journal of Hydrology, 362(1-2), 19-38.

Soares-Frazão, S., Lhomme, J., Guinot, V., Zech, Y. 2008. Two-dimensional shallow-water model with porosity for urban flood modelling. Journal of Hydraulic Research, 46(1), 45-64.

Soares-Frazão, S., Zech, Y. 2008. Dam-break flow through an idealised city. Journal of Hydraulic Research, 46(5), 648-658; DOI: 10.3826/jhr.2008.3164.

Spinewine, B., Capart, H., Larcher, M. & Zech, Y. 2003. Three-dimensional Voronoï imaging methods for the measurement of near-wall particulate flows. *Experiments in Fluids* 34 (2): 227-241.

Van Emelen, S. 2009. Ecoulements de crue en milieu urbain: développement et validation expérimentale d'un nouveau modèle de porosité. Msc dissertation (in French). Louvain-la-Neuve, Belgium.